Fluid-Elastic Coefficients in Single Phase Cross Flow: Dimensional Analysis, Direct and Indirect Experimental Methods

Romain Lagrange, Philippe Piteau, Xavier Delaune, Jose Antunes

FLUID-ELASTIC COEFFICIENTS IN SINGLE PHASE CROSS FLOW: DIMENSIONAL ANALYSIS, DIRECT AND INDIRECT EXPERIMENTAL METHODS

Romain Lagrange
DEN-Service d'Etudes Mécaniques et Thermiques
SEMT, CEA, Université Paris Saclay
F-91191 Gif-Sur-Yvette, France

Philippe Piteau
DEN-Service d'Etudes Mécaniques et Thermiques
SEMT, CEA, Université Paris Saclay
F-91191 Gif-Sur-Yvette, France

Xavier Delaune
DEN-Service d'Etudes Mécaniques et Thermiques
SEMT, CEA, Université Paris Saclay
F-91191 Gif-Sur-Yvette, France

Jose Antunes
Centro de Ciências e Tecnologias Nucleares
Instituto Superior Técnico, Universidade de Lisboa
Estrada Nacional 10, Km 139.7
2695-066 Bobadela LRS, Portugal

ABSTRACT

The importance of fluid-elastic forces in tube bundle vibrations can hardly be over-emphasized, in view of their damaging potential. In the last decades, advanced models for representing fluid-elastic coupling have therefore been developed by the community of the domain. Those models are nowadays embedded in the methodologies that are used on a regular basis by both steam generators providers and operators, in order to prevent the risk of a tube failure with adequate safety margins. From an R&D point of view however, the need still remains for more advanced models of fluid-elastic coupling, in order to fully decipher the physics underlying the observed phenomena. As a consequence, new experimental flow-coupling coefficients are also required to specifically feed and validate those more sophisticated models. Recent experiments performed at CEA-Saclay suggest that the fluid stiffness and damping coefficients depend on further dimensionless parameters beyond the reduced velocity.

In this work, the problem of data reduction is first revisited, in the light of dimensional analysis. For single-phase flows, it is underlined that the flow-coupling coefficients depend at least on two dimensionless parameters, namely the Reynolds number Re and the Stokes number Sk. Therefore, reducing the experimental data in terms of the compound dimensionless quantity $V_r = Re/Sk$ necessarily leads to impoverish results, hence the data dispersion. In a second step, experimental data are presented using the dimensionless numbers Re and Sk. We report experiments, for a 3x5 square tube bundle subjected to water transverse flow. The bundle is rigid, except for the central tube which is mounted on a flexible suspension allowing for translation motions in the lift direction. The evolutions of the flow-coupling coefficients with the flow velocity are determined using two different experimental procedures: (1) In the direct method, an harmonic motion of increasing frequency is imposed to the tube. (2) In the indirect method, the coefficients are obtained from the modal response of the tube (frequency, damping). The coefficient identification was performed well beyond the system instability boundary, by using active control, allowing an exploration of a significant range of flow velocity.

For a given Sk, the results show that: (a) at low Re, the flow-coupling coefficients are close to zero; (b) at intermediate Re, the flow stabilizes the tube; (c) at high Re, the flow destabilizes the tube, leading to a damping-controlled instability at a critical Re. Reducing the data in terms of Re and Sk clarifies the various experimental "branches", which are mixed when using V_r. The two identification techniques lead to reasonably compatible fluid-elastic coefficients.

NOMENCLATURE

$c_D = \dfrac{-2\widehat{C_f}}{\rho_f D L V_g}$	Dimensionless damping coefficient
$c_K = \dfrac{-2K_f}{\rho_f L V_g^{\,2}}$	Dimensionless stiffness coefficient
$c_T = \dfrac{C_s + C_f}{C_s + C_f^0}$	Dimensionless total damping coefficient
C_f	Fluid-added damping
C_f^0	Fluid-added damping in still fluid

$\widehat{C_f} = C_f - C_f^0$	Fluid-added damping due to fluid velocity
C_s	Structural damping of the moving tube
D	Tube diameter
F_a	Excitation fluid force
F_0	Frequency of first mode in still fluid
K_f	Fluid-added stiffness
K_s	Structural stiffness of the moving tube
L	Tube length
$l = L/D$	Tube aspect ratio
M_s	Structural mass of the moving tube
M_f	Fluid-added mass
P	Tube bundle pitch
$p = P/D$	Pitch ratio
$Re = DV_g/\nu$	Reynolds number
$Sk = D^2F_0/\nu$	Stokes number
$Sc = 2\pi\xi_0 \frac{M_s + M_f}{\rho_f D^2 L}$	Scruton number
V_g	Gap flow velocity
$V_r = V_g/(DF_0)$	Reduced velocity
X	Tube modal displacement
ρ_f	Mass density of the fluid
ν	Kinematic viscosity of the fluid
ξ_0	Damping of first mode in still fluid
λ	Characteristic length
M	Characteristic mass
τ	Characteristic time

INTRODUCTION

The knowledge of the fluid force acting on a structure subject to a cross flow is a crucial information that must be accounted for when designing heat-exchanger tube bundles. The large vibrations resulting from a fluid-elastic instability may lead to some mechanical degradation of the concerned tube, which may affect the power plant operation and safety. This instability can be described as a self-excited feedback mechanism between the motion of the structure and the fluid forces. Since the pioneering work of Tanaka and Takahara [1], several authors [2-10] measured the fluid-elastic force to feed the stability criterion models developed by Connors [11], Blevins [12], Chen [2,3], Lever and Weaver [13-15], Price and Païdoussis [16-18], Granger et al. [19,20] and Tanaka et al. [21]. Still, further experimental work is needed to accurately understand the effects of changing the tube mass, damping, frequency or diameter, as well as the bundle configuration, even for a single flexible tube within a rigid bundle subject to single-phase flow.

There are basically two techniques for obtaining the fluid-elastic force. The direct method [1,7-10] is based on imposing a controlled oscillatory motion to a given tube within a rigid bundle and measuring the forces exerted by the flow as a function of the flow velocity and of the motion frequency. The fluid-elastic force is obtained from the transfer function between the tube displacement and the measured force from which the structural inertia term is subtracted. The indirect method [4-6,22,23] applies to an instrumented tube, for which the fluid-elastic force is extracted from the changes in the modal frequency and damping of the vibrating tube. Both techniques have advantages and drawbacks, concerning the complexity of the setup, the sensitivity to external perturbations and the range of parameters that may be explored. Given all these constraints, an experimental rig allowing both measuring methods, as well as exploring beyond the instability threshold, has been developed at CEA, see [4-6, 22,23]. In this paper, we analyse these experimental results in the light of a dimensional analysis. In particular, we investigate the influence of the tube frequency and the water flow velocity on the fluid-elastic force.

DIMENSIONAL FLUID-ELASTIC COEFFICIENTS

We consider the vibration of a flexibly mounted tube (diameter D, length L), part of a 3x5 square tube bundle (pitch P), immerged in a viscous fluid of volume mass density ρ_f, kinematic viscosity ν and gap velocity V_g, see Fig. 1. We note M_s, C_s and K_s the mass, damping and rigidity coefficients of the first mode of vibration of the flexible tube in air. The modal displacement X in the lift direction is assumed to satisfy the equation:

$$\left(M_s + M_f\right)\ddot{X} + \left(C_s + C_f\right)\dot{X} + \left(K_s + K_f\right)X = F_a\,, \qquad (1)$$

where F_a is an excitation fluid force considered as independent on the tube motion. The modal frequency of the flexible tube in still water is

$$F_0 = \sqrt{K_s/\left(M_s + M_f\right)}\Big/(2\pi)\,. \qquad (2)$$

As most often assumed, we postulate that the added mass M_f does not depend on flow velocity, but only on fluid density and bundle geometry. In other words, M_f is an unknown function H_{M_f} of $\left(\rho_f, D, L, P\right)$:

$$M_f = H_{M_f}\left(\rho_f, D, L, P\right). \tag{3}$$

On the other hand, we consider that the fluid added damping C_f and rigidity K_f depend, at least, on the flexible tube frequency F_0, the fluid material properties ρ_f, ν, the gap velocity V_g, as well as the bundle geometry

$$C_f = H_{C_f}\left(F_0, \rho_f, \nu, V_g, D, L, P\right), \tag{4}$$

$$K_f = H_{K_f}\left(F_0, \rho_f, \nu, V_g, D, L, P\right). \tag{5}$$

Let C_f^0 be the fluid added damping coefficient in still fluid, defined as the value of C_f as $V_g = 0$. Then, $\widehat{C_f} = C_f - C_f^0$ is a measure of the effect of the fluid velocity V_g on the fluid added damping coefficient C_f, and is a function of $\left(F_0, \rho_f, \nu, V_g, D, L, P\right)$:

$$\widehat{C_f} = H_{\widehat{C_f}}\left(F_0, \rho_f, \nu, V_g, D, L, P\right). \tag{6}$$

The relations of dependence (3) to (6) constitute a minimal model, based on experimental observations, bibliography reporting and physical intuition. More advanced models would also consider the effect of some other parameters, for e.g. the roughness of the tubes.

DIMENSIONLESS FLUID-ELASTIC COEFFICIENTS

The dimensional analysis is based on the Vaschy-Buckingham theorem. The theorem states that an equation involving n physical variables with k fundamental units (usually $k = 3$ in classical mechanics) can be reduced to an equation involving $n-k$ dimensionless parameters. Thus, introducing a scale of length λ, mass M and time τ, the equations (3), (5) and (6) are physically meaningful if

$$\frac{M_f}{M} = H_{M_f}\left(\frac{\rho_f}{M\lambda^{-3}}, \frac{D}{\lambda}, \frac{L}{\lambda}, \frac{P}{\lambda}\right), \tag{7}$$

$$\frac{K_f}{M\tau^{-2}} = H_{K_f}\left(\frac{F_0}{\tau^{-1}}, \frac{\rho_f}{M\lambda^{-3}}, \frac{\nu}{\lambda^2\tau^{-1}}, \frac{V_g}{\lambda\tau^{-1}}, \frac{D}{\lambda}, \frac{L}{\lambda}, \frac{P}{\lambda}\right), \tag{8}$$

$$\frac{\widehat{C_f}}{M\tau^{-1}} = H_{\widehat{C_f}}\left(\frac{F_0}{\tau^{-1}}, \frac{\rho_f}{M\lambda^{-3}}, \frac{\nu}{\lambda^2\tau^{-1}}, \frac{V_g}{\lambda\tau^{-1}}, \frac{D}{\lambda}, \frac{L}{\lambda}, \frac{P}{\lambda}\right). \tag{9}$$

As (7) involves five dimensional quantities with two fundamental dimensions (length and mass), it can be reduced to a relation between three dimensionless quantities. Similarly, as (8) and (9) involve eight dimensional quantities with three fundamental dimensions (length, mass and time), they can be reduced to a relation between five dimensionless quantities. These dimensionless quantities are not unique and derive from a specific choice for the characteristic length λ, mass M and time τ. Picking $\lambda = D$, $M = \rho_f D^2 L$ and $\tau = D/V_g$, the dimensionless equations rewrite

$$\frac{M_f}{\rho_f D^2 L} = H_{m_f}\left(l, p\right), \tag{10}$$

$$c_K = \frac{-2K_f}{\rho_f L V_g^{\,2}} = H_{k_f}\left(V_r, l, Re, p\right), \tag{11}$$

$$c_D = \frac{-2\widehat{C_f}}{\rho_f D L V_g} = H_{c_f}\left(V_r, l, Re, p\right), \tag{12}$$

with $l = L/D$, $p = P/D$, $Re = DV_g/\nu$, and $V_r = V_g/DF_0$ the tube aspect ratio, the pitch ratio, the Reynolds number and the reduced velocity, respectively. In what follows, we shall also make use of the Stokes number, obtained from the ratio between Re and V_r: $Sk = Re/V_r = D^2F_0/\nu$. To study the stability of the tube, we introduce the total damping coefficient $c_T = \left(C_s + C_f\right)/\left(C_s + C_f^0\right)$, which also rewrites as

$$c_T = \frac{C_s + C_f^0 + \widehat{C_f}}{C_s + C_f^0} = 1 + \frac{\widehat{C_f}}{C_s + C_f^0} = 1 + \frac{c_D \rho_f D L V_g}{-2\left(C_s + C_f^0\right)}. \tag{13}$$

Introducing $Sc = 2\pi\xi_0\left(M_s + M_f\right)/\left(\rho_f D^2 L\right)$ and $\xi_0 = \left(C_s + C_f^0\right)/\left[2\left(M_s + M_f\right)\left(2\pi F_0\right)\right]$ as the Scruton number and the reduced damping parameter for a flexible tube in a still fluid, (13) simplifies to

$$c_T = 1 - \frac{c_D V_r}{4Sc} = H_{c_T}\left(V_r, l, Re, p, Sc\right). \tag{14}$$

It follows that the tube is stable if $c_T > 0$, unstable if $c_T < 0$ and the stability threshold $c_T = 0$ is a function of $\left(V_r, l, Re, p, Sc\right)$.

The above dimensionless analysis shows that the fluid-elastic coefficients c_D and c_K are not a function of V_r only, but also depend on the Reynolds number. The reduced velocity has the disadvantage to encapsulate both F_0 and V_g in a same

dimensionless number, whereas these two parameters are independent. Consequently, to distinguish the effect of the frequency and the fluid flow on the variation of the fluid-elastic coefficient, it is preferable to use the couple of dimensionless numbers (Sk, Re) instead of (V_r, Re). Adopting this point of view in the next sections, c_D and c_K are seen as functions of (Sk, l, Re, p). Similarly, the total damping coefficient c_T depends on (Sc, Sk, l, Re, p).

EXPERIMENTAL SETUP AND MEASUREMENT METHODS

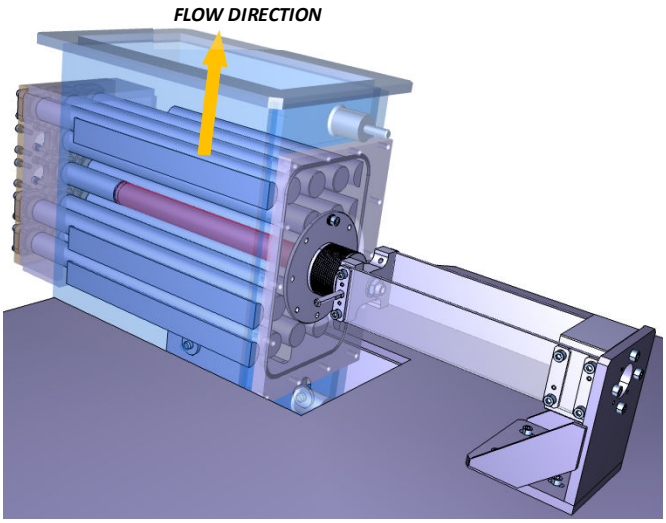

Figure 1. Bundle and flexibly mounted tube.

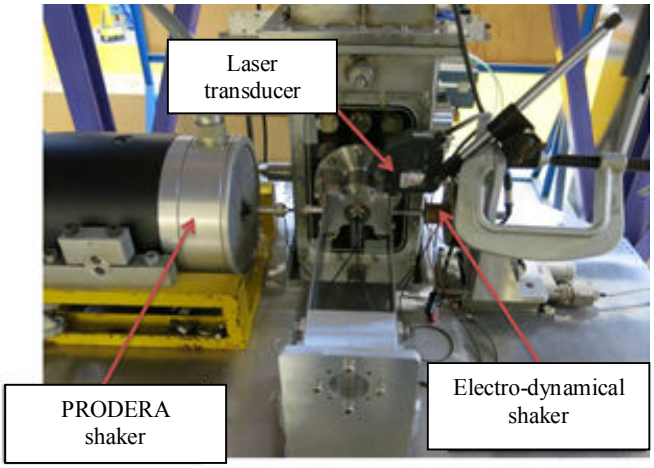

Figure 2. Experimental setup.

An experimental setup, has been built at CEA to study the variations of the fluid-elastic coefficients c_D and c_K. This experimental setup is sketched in figures 1 and 2 and described briefly in the following. Readers should refer to [4-6,22,23] for an extensive description. The tube bundle has immersed length $L = 300$ mm and diameter $D = 30$ mm, with a pitch ratio $P/D = 1.5$. As depicted in Fig. 1, the moving tube is in the central position of a 3×5 square bundle made of rigid tubes (plus two columns of 5 half-tubes at the boundaries). The central tube is supported by two parallel flexible steel blades allowing large vibrations in the lift direction. The tube bundle is subject to a cross water flow with a gap speed in the range $V_g = 0 \sim 6$ m/s. In terms of dimensionless numbers, this range of variation for V_g yields $Re = 0 \sim 10^5$. The fluid-elastic coefficients c_D and c_K are measured using two experimental approaches.

In the indirect method, the motion of the flexible tube is free and the measurement of its displacement and velocity is provided by a laser transducer (Keyence LK-G500). In order to investigate the variations of the fluid-elastic coefficients well beyond the stability threshold, a feedback control loop made of an electro-dynamical shaker was used, see [4-6,23]. The coefficients c_D and c_K are obtained from the variations of the tube motion frequency and damping. This technique for extraction of the fluid-elastic coefficients from the modal parameters is simple and proved robust enough. Since three coefficients are to be extracted from only two modal parameters, the assumption of a constant added mass (e.g. a velocity-independent flow inertia coefficient) has to be somewhat arbitrarily enforced, which is a disadvantage of this identification method. Any possible changes in M_f due to the fluid velocity will then be reflected in the coupling coefficient K_f. The modal frequency of the moving tube is set by changing the thickness of the blades or by adding a suitable mass to the moving fixture. Several configuration tests, denoted L1, L2, L3, L3B, L4B and L4TI, see Table 1, have been performed, covering a large range of frequencies $F_0 \approx 13 \sim 39$ Hz. The second modal frequency is much larger than F_0, such that the tube dynamics is mainly a rigid translation.

In the direct method, an harmonic motion of imposed frequency is directly applied to the tube, thanks to a PRODERA shaker, see Fig. 2. The fluid force acting on the flexible tube is only measured in the lift direction with a KISTLER sensor. The coefficients c_D and c_K are directly extracted from the measure of the fluid force. This method, first introduced by Tanaka in the 80's and mainly followed by Chen in the 90's has yield some interesting results. However, despite its apparent simplicity, it has been progressively abandoned due to its difficult experimental implementation. Three measurement campaigns,

denoted L1TI 2017, L1TI 2018 and L3TI have been conducted, with imposed frequencies covering the range $F_0 \approx 13 \sim 39$ Hz .

TEST	$\frac{M_s + M_f}{L}$ $(\mathrm{kg.m^{-1}})$	ξ_0 (%)	F_0 (Hz)	Scruton Sc $(\times 10^{-1})$	Stokes Sk $(\times 10^{4})$
L1	3.77	0.90	12.99	2.36	1.169
L2	4.57	1.19	26.47	3.78	2.382
L3	5.17	0.71	38.58	2.57	3.472
L3B	6.77	0.69	33.72	3.27	3.035
L4	4.17	0.64	20.76	1.86	1.868
L4B	6.10	0.62	17.47	2.64	1.572
L4TI	5.33	0.61	18.40	2.27	1.656

Table 1. Tested configurations. Indirect method.

EXPERIMENTAL RESULTS

In this section, we present the experimental measurements of c_D , c_K and c_T , obtained from the indirect and direct methods. We focus on the evolution of these dimensionless coefficients with the Reynolds and the Stokes numbers. On the following figures, curves with identical colours correspond to configuration tests with similar Stokes numbers, see Table 1.

The measurements of c_D obtained from the indirect method are shown in Fig. 3. Whatever the Stokes number, a clear general trend is observed. At low Reynolds numbers, $c_D \approx 0$, such that the fluid velocity has a negligible effect on the stability of the tube. At intermediate Reynolds numbers, c_D becomes negative such that the tube is getting stabilized. In this range of Re , some kinetic energy is conveyed by the vibrating tube to the fluid, which in turn propagates this energy through the far domain. This corresponds to an energy loss for the tube leading to a damping of its vibrations. It is believed that the energy propagation through the far domain is enhanced by some fluid vortices whose existence still needs to be proven. At high Reynolds numbers, c_D increases and the tube becomes unstable for some critical Re_c , corresponding to $c_T = 0$. In this range of Re , some elastic and kinetic energy is conveyed by the fluid motion to the tube. This corresponds to an energy gain for the tube whose vibrations are amplified. In this range, we note that c_D decreases with the Stokes number Sk , such that a tube with a high frequency is more stable than a tube with a low frequency.

In figures 4, 5 and 6, we compare the measurements of c_D obtained from the indirect method and the direct method. For $Sk \approx 1{,}169 \times 10^4$ (i.e. $F_0 \approx 13$ Hz , figure 4) and $Sk \approx 1{,}7 \times 10^4$ (i.e. $F_0 \approx 18$ Hz , figure 5) the two methods yield similar experimental results. For $Sk \approx 2{,}382 \times 10^4$ (i.e. $F_0 \approx 26$ Hz , figure 6), significant differences are observed, especially at low Reynolds numbers. We attribute these differences to a bad signal to noise ratio due to some parasitic frequencies in the experimental setup as the forcing frequency F_0 of the direct method is increased. Also, at high forcing frequencies, the precise determination of the fluid-elastic force is complicated as most of the measured force has an inertia origin.

The measurements of c_K obtained from the indirect method are shown in Fig. 7. At low Reynolds numbers, the data are scattered and difficult to analyze in the sense that no special trend is clearly observed. However, if the fluid velocity has a negligible effect on the dynamics of the structure, as it is believed from the analysis of c_D , then one would expect that $c_K \approx 0$. At intermediate Reynolds numbers, c_K becomes positive such that the relative rigidity of the tube diminishes. As already pointed out, this could be related to the existence of some fluid vortices interacting with the structure. At high Reynolds numbers, c_K decreases such that the relative rigidity of the tube is enhanced. Still, c_K being positive, the total rigidity $K_s + K_f$ of the tube in a flowing fluid is smaller than its rigidity K_s in a fluid at rest. Thus, in this range of Re , the frequency of the tube vibrations is smaller than F_0 .

The evolution of the total damping coefficient c_T is shown in Fig. 8. The variations of this coefficient are directly related to those of c_D through the equation (14). Consequently, at low Reynolds numbers, $c_D \approx 0$ yields $c_T \approx 1$. In this range of Re the fluid velocity does not affect the stability of the structure. At intermediate Reynolds numbers, c_T increases (i.e. c_D decreases), meaning that the tube loses some energy and gets stabilized. At high Reynolds numbers, c_T decreases (i.e. c_D increases) meaning that the tube is gaining some energy from the fluid, leading to amplified vibrations. Eventually, at a critical Reynolds number Re_c , the total damping coefficient vanishes and the tube becomes unstable. The figure 8 clearly shows that the stability threshold Re_c increases with the Stokes

number Sk . The determination of the exact relation between Re_c and Sk is however difficult from the present experimental results as the configuration tests listed in Table 1 do not have exactly the same Scruton numbers. Still, we show in figure 9 that the representation of c_T versus the reduced velocity $V_r = Re/Sk$ does not yield a collapse of the experimental data on a master curve, in particular close to the stability threshold $c_T = 0$. In other words, the flow-coupling coefficients do not only depend on V_r, and contrarily to the prediction of Connors [11], Re_c is probably not a linear function of Sk .

Finally, the dependence of the fluid-elastic coefficients with the Stokes number might be explained by several physical reasons. The most likely one is that the flow regime might be triggered by the tube frequency. The tube frequency might also affect the time-lag between the tube motion and the fluid forces. Whatever the physical explanation, the results presented suggest a strong dependence on both the flow Reynolds number and the Stokes number, beyond the classicaly assumed dependence on the reduced velocity.

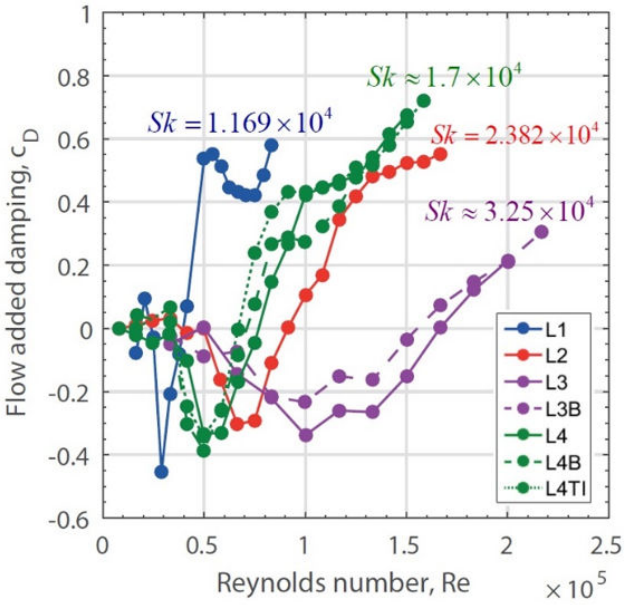

Figure 3. Evolution of the flow added damping coefficient c_D with the Reynolds and the Stokes numbers. Indirect method.

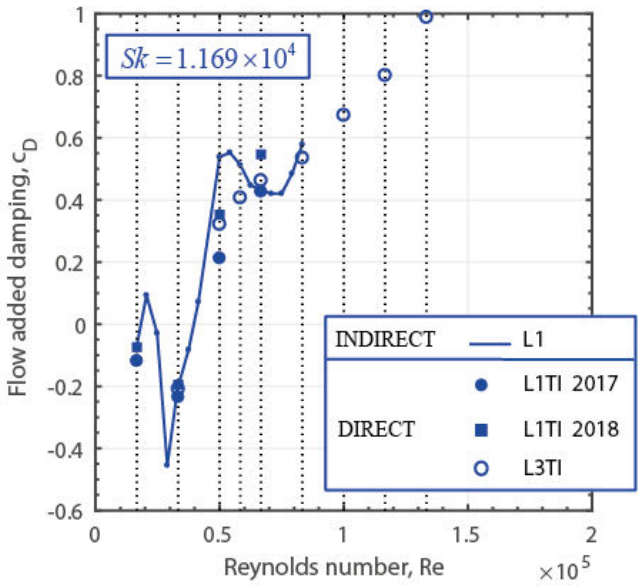

Figure 4. Evolution of the flow added damping coefficient c_D with the Reynolds number.

Indirect and direct methods. $Sk = 1.169 \times 10^4$.

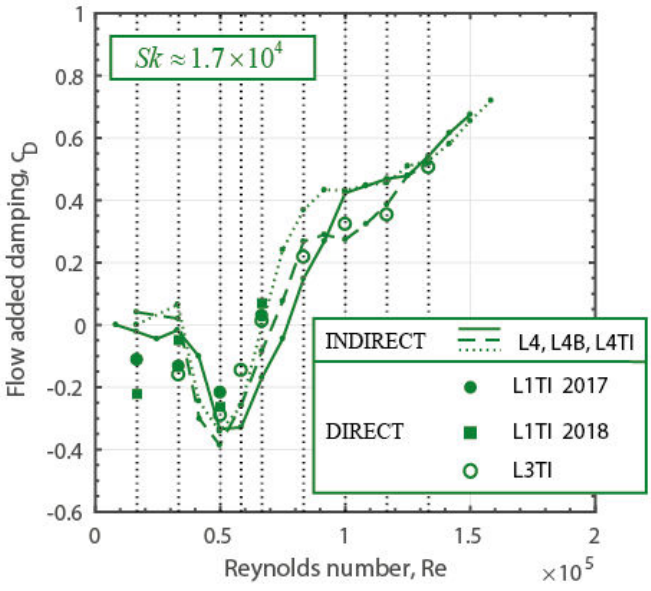

Figure 5. Evolution of the flow added damping coefficient c_D with the Reynolds number.

Indirect and direct methods. $Sk = 1.7 \times 10^4$.

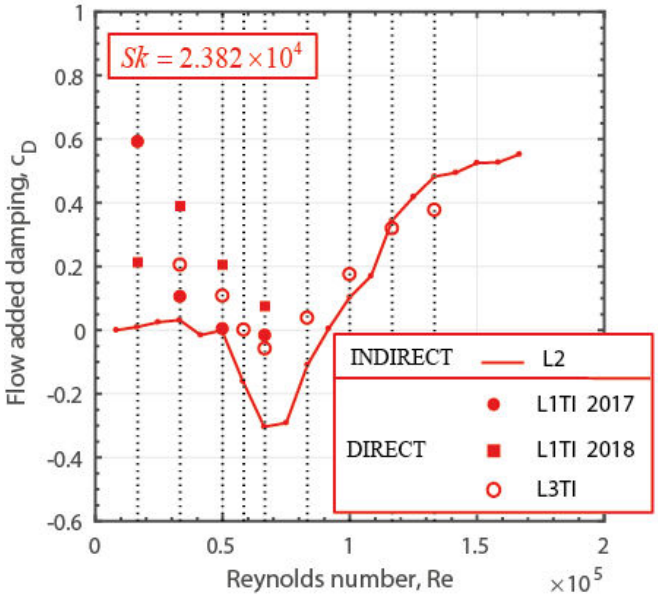

Figure 6. Evolution of the flow added damping coefficient c_D with the Reynolds number.
Indirect and direct methods. $Sk = 2.382 \times 10^4$.

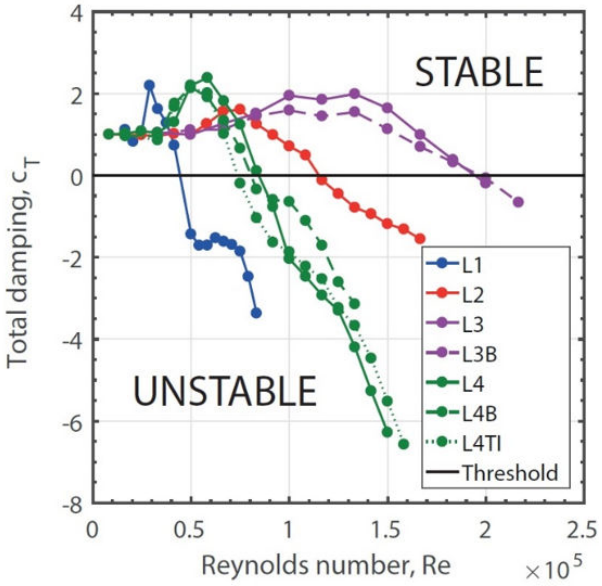

Figure 8. Evolution of the total damping coefficient c_T with the Reynolds and the Stokes numbers. Indirect method.

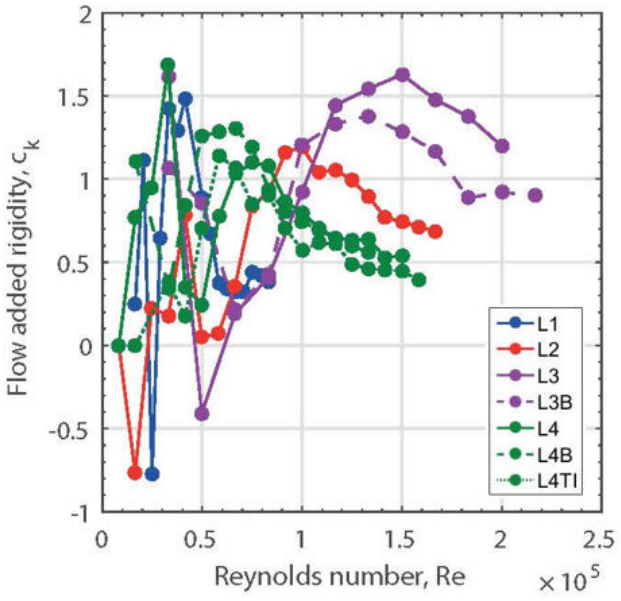

Figure 7. Evolution of the flow added rigidity coefficient c_K with the Reynolds and the Stokes numbers. Indirect method.

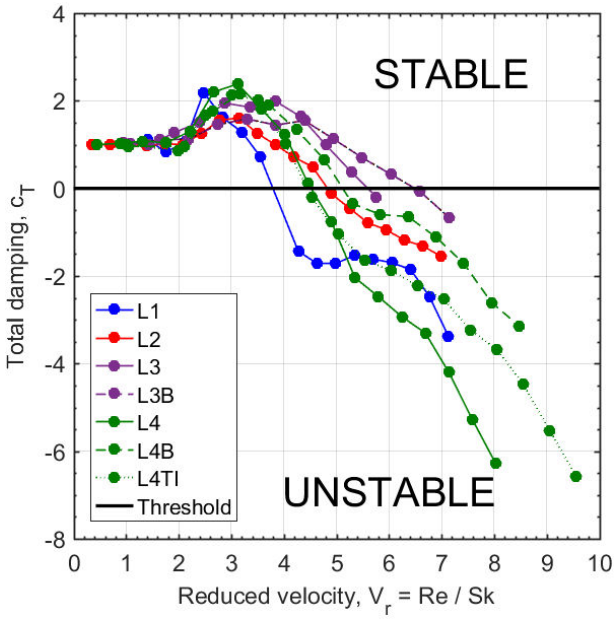

Figure 9. Evolution of the total damping coefficient c_T with the reduced velocity and the Stokes number. Indirect method

CONCLUSIONS

In this work, we have studied the lift vibration of a flexible tube subject to a single phase cross flow. The flexible tube is located in the central position of a square rigid tube bundle. A dimensional analysis shows that the fluid-elastic coefficients are not a function of the reduced velocity only, but also depend on the Reynolds number. This observation is confirmed in our experiments by using two different methods of measurement. In the direct method, an harmonic motion of increasing frequency is imposed to the tube. In the indirect method, the coefficients are obtained from the changes in tube vibration frequency and damping. Both methods suggest the existence of three different dynamics for the flexible tube. At low Reynolds numbers, the fluid velocity has no effect on the stability of the tube. At moderate Reynolds numbers, the tube loses some energy and gets stabilized. At large Reynolds numbers, the tube gains some energy from the fluid and becomes unstable at a critical Reynolds. The experiments show that a tube with a high frequency is more stable than a tube with a low frequency.
Finally, it shall be noted that some significant differences are observed in comparing the results of measurement from the two experimental methods as the Stokes number is increased and as the Reynolds numbers is decreased (i.e. low reduced velocities). We attribute these differences to a bad signal to noise ratio due to some parasitic frequencies in the experimental setup as the forcing frequency of the direct method is increased. Still, these first comparisons are very encouraging and should foster further developments of the direct method.

ACKNOWLEDGMENTS

The authors acknowledge financial support for this work, which was performed in the framework of a joint research program co-funded by FRAMATOME, EDF and CEA (France).

REFERENCES

[1] Tanaka H., Takahara S. (1981), "Fluidelastic Vibration of Tube Arrays in Cross-Flow", *Journal of Sound and Vibration*, Vol. 77, pp. 19-37.

[2] Chen S.S. (1983), "Instability Mechanisms and Stability Criteria of a Group of Circular Cylinders Subjected to Cross-flow. Part 1: Theory", *Journal of Vibration, Acoustics, Stress and Reliability in Design*, Vol. 105, pp. 51-58.

[3] Chen S.S. (1983), "Instability Mechanisms and Stability Criteria of a Group of Circular Cylinders Subjected to Cross-flow. Part 2: Numerical Results and Discussion", *Journal of Vibration, Acoustics, Stress and Reliability in Design*, Vol. 105, pp. 253-260.

[4] Caillaud S., de Langre E., Piteau P. (1999), "The Measurement of Fluidelastic Effects at Low Reduced Velocities Using Piezoelectric Actuators", *ASME Journal of Pressure Vessel Technology*, Vol. 121, pp. 232-238.

[5] Caillaud S., de Langre E., Piteau P. (2000), "Measurement of Critical Velocities for Fluidelastic Instability Using Vibration Control", *ASME Journal of Vibration and Acoustics*, Vol. 122, pp. 341-345.

[6] Caillaud S., de Langre E., Baj F. (2003), "Active Vibration Control for the Measurement of Fluidelastic Effects", *ASME Journal of Pressure Vessel Technology*, Vol. 125, pp. 165-170.

[7] Mureithi N.W., Nakamura T., Hirota K., Murata M., Utsumi S., Kusakabe T., Takamatsu H. (2002), "Dynamics of an Inline Tube Array Subjected to Steam-Water Cross Flow. Part 2: Unsteady Fluid Forces", *Journal of Fluids and Structures*, Vol. 16, pp. 137–152.

[8] Inada F., Kawamura K., Yasuo A., Yoneda K. (2002), "An Experimental Study on the Fluidelastic Forces Acting on a Square Tube Bundle in Two-Phase Cross Flow". *Journal of Fluids and Structures*, Vol. 16, pp. 891–907.

[9] Sawadogo T., Mureithi N.W., (2014), "Fluidelastic Instability Study in a Rotated Triangular Tube Array Subject to Two-Phase Cross-Flow. Part 1: Fluid Force Measurements and Time Delay Extraction", *Journal of Fluids and Structures*, Vol. 49, pp. 1-15.

[10] Sawadogo T., Mureithi N.W. (2014), "Fluidelastic Instability Study in a Rotated Triangular Tube Array Subject to Two-Phase Cross-Flow. Part 2: Experimental Tests and Comparison with Theoretical Results", *Journal of Fluids and Structures*, Vol. 49, pp. 16-28.

[11] Connors H.J. (1970), "Fluidelastic Vibration of Tube Arrays Excited by Cross-Flow", *Proc. Flow-Induced Vibration in Heat-Exchangers* (Reiff, D.D. Ed), ASME, pp. 42-56.

[12] Blevins R.D. (1974), "Fluidelastic Whirling of a Tube Row", *Journal of Pressure Vessel Technology*, Vol. 96, pp. 263-267.

[13] Lever J.H, Weaver D.S. (1982), "A Theoretical Model for the Fluidelastic Instability in Heat Exchanger Tube Bundles", *ASME Journal of Pressure Vessel Technology*, Vol. 104, pp. 147-158.

[14] Lever J.H., Weaver D.S. (1986), "On the Stability of Heat Exchanger Tube Bundles. Part 1: Modified Theoretical Model", *Journal of Sound and Vibration*, Vol. 107, pp. 375-392.

[15] Lever J.H., Weaver D.S. (1986), "On the Stability of Heat Exchanger Tube Bundles. Part 2: Numerical Results and Comparison with Experiments", *Journal of Sound and Vibration*, Vol. 107, pp. 375-392.

[16] Price S.J., Païdoussis M.P. (1983), "Fluidelastic Instability of an Infinite Double Row of Circular Cylinders Subject to a Uniform Cross-Flow", *Journal of Vibration, Acoustics, Stress and Reliability in Design*, Vol. 105, pp. 59–66.

[17] Price S.J., Païdoussis M.P. (1984), "Improved Mathematical Model for the Stability of Cylinder Rows Subject to Cross-Flow", *Journal of Sound and Vibration*, Vol. 97, pp. 615–640.

[18] Païdoussis M.P., Price S.J. (1988), "The Mechanisms Underlying Flow-Induced Instabilities of Cylinder Arrays in Cross-Flow", *Journal of Fluid Mechanics*, Vol. 187, pp. 45–59.

[19] Granger S., Campistron R., Lebret J. (1993), "Motion-Dependent Excitation Mechanisms in a Square In-Line Tube Bundle Subject to Water Cross-Flow: An Experimental Modal Analysis", *Journal of Fluids and Structures*, Vol. 7, pp. 521-550.

[20] Granger S., Païdoussis M.P. (1996), "An Improvement to the Quasi-Steady Model with Application to Cross-Flow-Induced Vibration of Tube Arrays", *Journal of Fluid Mechanics*, Vol. 320, pp. 163–184.

[21] Tanaka H., Tanaka K., Shimizu F., Takahara S. (2002), "Fluidelastic Vibration of Tube Arrays in Cross-Flow", *Journal of Fluids and Structures*, Vol. 16, pp. 93-112.

[22] Piteau P., Delaune X., Antunes J, Borsoi L. (2012), "Experiments and Computations of a Loosely Supported Tube in a Rigid Bundle Subjected to Single-Phase Flow", *Journal of Fluids and Structures*, Vol. 28, pp. 56-71.

[23] Piteau P., Delaune X.,Borsoi L.,Antunes J. (2019), "Experimental identification of fluid-elastic coupling forces on a flexible tube within a rigid square bundle subjected to single-phase cross-flow", *Journal of Fluids and Structures*, Vol. 86, pp. 156-169.